Received Date : 22-Aug-2016

Revised Date : 17-Oct-2016

Accepted Date : 22-Oct-2016

Article type : Research Article

Running head: Design and synthesis of CAMKIV inhibitors

Design, synthesis and biological evaluation of pyrimidine derivatives as potential inhibitors of human CAMKIV

Ehtesham Jameel[1,†], Huma Naz[2,†], Parvez Khan[2], Mohd. Tarique[3], Jitendra Kumar[4], Syed Mumtazuddin[1], Shahzaib Ahamad[5], Asimul Islam[2], Faizan Ahmad[2], Nasimul Hoda[4,*] and Md. Imtaiyaz Hassan[2,*]

[1]*Department of Chemistry, B.R. Ambedkar Bihar University, Muzaffarpur 842001, Bihar, India.*

[2]*Centre for Interdisciplinary Research in Basic Sciences, Jamia Millia Islamia, New Delhi-110025, India.*

[3] *Department of Biochemistry, All India Institute of Medical Sciences, New Delhi-110029, India.*

[4]*Department of Chemistry, Jamia Millia Islamia, New Delhi 110025, India.*

[5]*Department of Biotechnology, College of Engineering & Technology, IFTM, Lodhipur-Rajput, Delhi Road, Moradabad, India.*

[†]*Equally Contributed*

Correspondence

Dr. Nasimul Hoda
(Associate Professor)
Department of Chemistry
Jamia Millia Islamia, New Delhi-110025
E-mail: nhoda@jmi.ac.in

Dr. Md. Imtaiyaz Hassan
(Assistant Professor)
Centre for Interdisciplinary Research in Basic Sciences,
Jamia Millia Islamia, New Delhi-110025
E-mail: mihassan@jmi.ac.in

Abstract

Calcium/calmodulin-dependent protein kinase IV (CAMKIV) is a multi-functional Ser/Thr kinase, associated with cerebral hypoxia, cancer and neurodegenerative diseases. Here, we report design, synthesis and biological evaluation of seven pyrimidine substituted novel inhibitors of CAMKIV. We successfully synthesized and extensively characterized (ESI-MS, ^{1}H NMR and ^{13}C NMR studies) seven compounds which are showing appreciable binding-affinity to the CAMKIV. Molecular docking and florescence binding studies revealed that compound 1 is showing very high binding free energy (ΔG =–11.52 kcal/mol) and binding-affinity (K= 9.2 x 10^{10} M^{-1}) to the CAMKIV. We further performed MTT assay to check the cytotoxicity and anti-cancer activity of these compounds. An appreciable IC_{50} (39μM) value of compound 1 was observed on human hepatoma cell line and non-toxic till the 400 μM on human embryonic kidney cells. To ensure anticancer activity of all these compounds, we further performed propidiumiodide assay to evaluate cell viability and DNA content during the cell cycle. We found compound 1 is again showing a better anticancer activity on both human hepatoma and human embryonic kidney cell lines.

Keywords: Calcium/calmodulin-dependent protein kinase IV; drug design and discovery; molecular docking; high affinity ligands; anticancer activity

Introduction

Protein kinases are the group of enzymes which comprise of 2% genes of eukaryotic genomes [1]. These kinases play key roles in the regulation of cellular functions via phosphorylation [2], and thus considered as a potential drug target for numerous diseases [3]. In the last 15 years, many pharmaceutical industries made a tremendous effort to synthesize small molecule kinase inhibitors for therapeutic applications [2, 4-7]. Calcium/calmodulin-dependent protein kinase IV (CAMKIV) is a 473 amino acid residues long nuclear protein kinase which belongs to the Ser/Thr kinase family [8, 9]. It is a multifunctional protein, expressed in the neuron in plenty [10, 11], while in spleen and testis its expression is scant [12]. Regulation of this kinase is depending on calcium signal cascade through phosphorylation of the substrate, thus CAMKIV plays a pivotal role in various cellular processes such as cell cycle regulation, apoptosis, cell signaling, progression and differentiation by regulating different transcription factors [13, 14]. CAMKIV activates nuclear CREB through phosphorylation on its residue Ser133 [15-17] followed by the phosphorylation of transcription activator CREB-binding protein (CBP). Such binding leading to the activation of CRE-mediated transcription through mobilization of CBP to the promoter which regulates transcription [17, 18]. Activation mechanism of CAMKIV is a tightly controlled process. Mutation, over-expression, synaptic and hormonal stimuli fasten neurodegenerative diseases, immunological disorders and hepatic [19], epithelial ovarian [20] and lung cancers [21].

Since, CAMKIV is directly involved in the regulation of several cellular processes, therefore, synthesis of small molecule inhibitors could help to regulate several activation pathways and signaling processes [22]. Recently, potent CaMKII inhibitors such as STO609, KN-93 [23] and KN-62 [24] are reported. STO609 kinase inhibitor was used to determine nucleocytoplasmic shuttling of high mobility group box 1 protein by the serine phosphorylation of CAMKIV during lipopolysaccharide (LPS)-induced stimulation of macrophages [25]. On the other hand, KN-93 is used for the treatment of nephritic syndrome which is responsible for kidney diseases like glomerulosclerosis, diabetes mellitus, focal segmental and systemic lupus erythematosus. Both KN-93 and KN-62 are competitively inhibiting the interaction of CAMK to Ca-calmodulin complex, and subsequently affecting the voltage-gated Ca^{+} or K^{+} ion channels, which resulting in the loss of cellular functions [26]. All these kinase inhibitors have been proven as significant tool for drug targeting but due to their off side targeting, specificity of kinases and failure of many drugs in phase III trial causing hurdle for pharmaceutical industries [27].

Structure-based drug design is the design and utilizes structural information of any target protein to optimize the chemical structure of inhibitors/ligands with a goal to identify a compound suitable for clinical testing (or drug molecule) [28-35]. Recently, we have synthesized few pyrimidine substituted compounds which showed inhibition of CAMKIV and possesses anticancer activity as well [36, 37]. In search of better inhibitors, we generated 100 compounds through chemical modifications on a pyrimidine scaffold which may be considered as potential inhibitors of CAMKIV. We performed docking studies on 7 synthesizable lead molecules which were showing an appreciable binding affinities to the CAMKIV. All selected molecules were successfully synthesized and characterized by ESI-MS, CHNS, ^{1}H and ^{13}C NMR. Binding

affinities of these molecules were further measured by fluorescence. Finally, anticancer activities of these compounds were evaluated through MTT and propidium iodide (PI) assays.

Materials and Methods

Materials

Media for bacterial culture Luria broth and Luria agar were purchased from Himedia (Mumbai, India). Agarose was purchased from Biobasic (Ontario, Canada). Restriction enzymes (*NdeI* and *XhoI*), PCR-*Taq*DNA polymerase and phusion polymerase, cloning-quick DNA ligase were purchased from Invitrogen BioServices India. Ni-NTA column was purchased from Genetix Biotech Asia (New Delhi, India). Reagent and solvents for chemical synthesis were purchased from Merck, Spectrochem and SD fine chemicals, India. Human hepatoma (HuH7) and human embryonic kidney (HEK293) cell lines were procured from National Centre for Cell Sciences, Pune, India. Antibiotic cocktail, fetal bovine serum and Dulbecco's modified eagle's media were purchased from Gibco-life technologies. Propidium iodide was purchased from Thermo Fisher Scientific (USA). MTT (3-[4,5-dimethylthiazol-2-yl]-2,5-diphenyltetrazolium bromide), trypsin-EDTA solution and PMSF were purchased from Sigma (St. Louis, MO).

Methods

Protein expression and purification

CAMKIV protein was successfully expressed into BL21(λE3) strain of *E. coli* and purified in its denatured form using slight modification of our reported procedure [36, 38, 39].

Docking Studies

The docking and scoring of ligands with CAMKIV protein was accomplished using ParDOCK module of *Sanjeevini* drug design suite which is based on physico-chemical descriptors [40]. We used the atomic coordinates of CAMKIV modeled previously [36]. Ligand molecules designed by chemical modifications of pyrimidine scaffold are listed in the **Supplementary Table S1**. We used a rigid docking module computed in several computational steps including preparation of reference protein complex and ligand in a force-field compatible manner as an input file. Docking of ligand molecule at the active site cavity of CAMKIV was done by using all atom energy based Monte Carlo algorithm which minimizes and scores the docked complex. The docked complexes were further minimized using the parallel version of sander module of AMBER [41], predicted binding free energy of docked poses are obtained using Bappl/BapplZ scoring function [42]. The crystal structure of complex, CAMKIV protein in complex with 4-Amino (sulfamoyl-phenylamino)-triazole-carbothioic acid (2,6-difluoro-phenyl)-amide) (PDB ID 2W4O) was utilized as reference.

Chemistry

All reagents were purchased from Merck and Spectrochem Co., and were purified and dried according to usual procedure. The anhydrous solvents used in synthesis were dried prior to use. Thin-layer chromatography (TLC) was performed on (0.25 mm silica gel 60 F254, Merck, Germany) pre coated aluminum sheet and spots were visualized under UV light to monitor the reactions. Separation and purification of all synthesized compounds were done by using column chromatography on silica gel 60-120 mesh, Merck. Melting points were determined on Veego melting point instrument (REC-22038 A2). NMR spectra were run in a solution of $CDCl_3$ or DMSO-d_6 and were recorded on (Bruker's AVANCE-III 400 MHz and Bruker DPX 300 MHz FT NMR spectrometers), with tetra methyl silane (TMS) as an internal standard and were recorded in parts per million (ppm). ^1H and ^{13}C NMR spectra were obtained at 400/100 MHz ($^1H/^{13}C$) and 300/75 MHz ($^1H/^{13}C$). ESI-MS were determined on Applied Biosystem (ABSCIEX-2000 Triple quad) spectrometer.

Synthesis of 8-((6-chloropyrimidin-4-yl)oxy)quinoline [Compound 1]

Solid 4,6-dichloropyrimidine (5 g, 1.2 equiv.) was added to a stirred solution of 8-hydroxyquinoline (4 g) and K_2CO_3 (5.7 g, 1.5 equiv.) in anhydrous DMF (40 mL), and the mixture was stirred overnight at room temperature (r.t.). After the completion of reaction (monitored by TLC), water was added and the organic compounds were extracted with EtOAc (3×60mL). The combined organic layers were washed with brine and dried over anhydrous Na_2SO_4 which was concentrated on reduced pressure to obtain the crude brown oil. The resulting crude oil was purified by silica gel column chromatography, EtOAc/Hexane (20:80 v/v) to obtain **compound 1** a pure white solid; yield 81%; m.p. 158 ºC; ^1H-NMR(300 MHz, $CDCl_3$) δ 8.82 (dd,

J = 3.9, 1.2 Hz, 1H), 8.44 (s, 1H), 8.22 (dd, *J* = 8.4, 1.2 Hz, 1H), 7.80 (d, *J* = 6.9 Hz, 1H), 7.59 (d, *J* = 8.1 Hz, 1H), 7.56 (d, *J* = 0.9 Hz, 1H), 7.44 (m, 1H), 7.13 (s, 1H); ^{13}C-NMR (75 MHz, $CDCl_3$) δ 170.92, 161.77, 158.28, 150.52, 148.36, 141.06, 136.17, 129.84, 126.43, 126.35, 121.93, 121.37, 108.05; ESI-MS: m/z = 258.4 [M^++H].

Representative procedure for the synthesis of 4-Methyl-7-hydroxycoumarin

Concentrated H_2SO_4 (100 ml) was added to a 250 mL round flask and cooled in an ice bath at 0 °C. A solution of resorcinol (10g, 1equiv.) in ethyl aceto-acetate (12mL,1equiv.) was added drop-wise to the flask with constant stirring and the temperature was kept below 10°C. The contents were stirred overnight at room temperature. Then, the reaction mixture was poured onto crushed ice with vigorous stirring. A solid product that formed instantly was filtered under suction and washed with copious amounts of cold water. The raw material was recrystallized from ethanol to obtain pure 4-Methyl-7-hydroxycoumarin with an approximately 70% yield [43].

Synthesis of 7-[(6-chloropyrimidin-4-yl)oxy]-4-methyl-2H-chromen-2-one [Compound 2]

A solution of 7-hydroxy-4-methylcoumarin (4.2g, 1.2equiv.) was added slowly to the solution of 4,6-dichloropyrimidine (3g) and K_2CO_3 (3.6g, 1.3equiv.) in dry DMF (60mL). The reaction mixture was stirred at r.t. for 5-6hrs and monitored by TLC. The precipitate formed was filtered, washed with plenty of cold water and recrystallized from DCM to obtain **compound 2** as a pure off white solid; yield 63%; m.p=196 ºC; ^{1}H-NMR (400 MHz, $CDCl_3$) δ 8.56 (s, 1H), 7.66 (d, *J* = 8.8 Hz, 1H), 7.15 (s, 1H), 7.10 (d, *J* = 10.8 Hz, 1H), 7.02 (s, 1H), 6.28 (d, *J* = 0.8 Hz, 1H), 2.44 (s, 3H, For -CH_3);^{13}C-NMR (100 MHz, $CDCl_3$) δ 169.48, 162.40, 160.27, 158.41,154.47,

154.29, 151.81, 125.87, 118.17, 117.84, 114.74, 110.40, 108.51, 18.76; ESI-MS: m/z =288.8 $[M]^+$.

Synthesis of 6-chloro-N-(4-methoxyphenyl)pyrimidin-4-amine [Compound 3]

A mixture of 4,6-dichloropyrimidine (4.0g), *p-anisidine* (3.3g, 1equiv.) and *N,N-Diisopropylethylamine* (DIPEA) (4.8mL, 1equiv.) was stirred at r.t. for 2-3 hrs and diluted with water. The formed solid was triturated with water and collected by filtration followed by diethyl ether and hexane (2:8) to obtain the desired intermediate **compound 3** as light green solid; Yield 74%; m.p. 135 ºC; ^{1}H NMR (300 MHz, $CDCl_3$) δ 8.38 (s, 1H, Ar), 7.45 (s, 1H, -NH), 7.21 (d, *J* = 7.5 Hz, 2H, Ar), 6.96 (d, *J*=7.5 Hz, 2H, Ar), 6.51 (s, 1H, Ar), 3.84 (s, 3H, -OCH_3); ^{13}C NMR (75 MHz, $CDCl_3$) δ 163.06, 160.45, 158.53, 158.15, 129.59, 125.98, 115.06, 102.05, 55.55; ESI-MS: m/z = 236.2 [M^++H].

Synthesis of 8-((6-(naphthalen-2-yloxy)pyrimidin-4-yl)oxy)quinoline [Molecule 1]

To a mixture of (compound 1**;** 0.75g) and K_2CO_3 (0.4 g; 1.5equiv.) in anhydrous DMF under N_2 medium, β-naphthol (0.41 g; 1equiv.)was added slowly at r.t. and the reaction mixture was reflux overnight. After the completion of reaction (monitored by TLC), the reaction mixture was allowed to cool at r.t. and extracted with EtOAc (3×40mL). The organic layer was washed with water, brine, dried over Na_2SO_4 and evaporated at reduced pressure to yield the crude product which was purified by column chromatography eluted with EtOAc/Hexane (80:20 v/v) to give pure final compound **Molecule 1** as honey color viscous liquid; yield 64%; ^{1}H-NMR (300 MHz, $CDCl_3$) δ 8.87 (dd, *J* = 4.2, 1.8 Hz, 1H, Ar), 8.33 (s, 1H, Ar), 8.19 (dd, *J* = 8.4, 1.5 Hz, 1H, Ar), 7.88 (s, 1H, Ar), 7.83 (d, *J* = 3.9 Hz, 1H, Ar), 7.80 (s, 1H, Ar), 7.76 (d, *J* = 6.0 Hz, 1H, Ar), 7.63

(d, *J* = 2.1 Hz, 1H, Ar), 7.58 (s, 1H, Ar), 7.53 (d, *J* = 1.8 Hz, 1H, Ar), 7.50 – 7.46 (m, 2H, Ar), 7.42 (d, *J* = 4.2 Hz, 1H, Ar), 7.32 (dd, *J* = 9.0, 2.4 Hz, 1H, Ar), 6.58 (d, *J* = 0.6 Hz, 1H, Ar);^{13}C-NMR (75 MHz, CDCl3) δ 172.23, 171.76, 158.19, 150.50, 150.26, 148.84, 141.50, 136.17, 134.07, 131.50, 129.93, 127.90, 127.66, 126.74, 126.47, 126.01, 125.81, 121.83, 121.55, 121.26, 118.45, 92.53, 60.38;ESI-MS: m/z = 366.0 [M^++H], 367.0 [(M+2H)]$^+$; Elemental Anal. Calcd for $C_{23}H_{15}N_3O_2$: C, 75.60; H, 4.14; N, 11.50; O, 8.76; Found: C, 75.90; H, 4.99; N, 11.89.

Synthesis of 8-((6-((5-methoxy-1H-benzo[d]imidazol-2-yl)thio)pyrimidin-4-yl)oxy)quinoline [Molecule 2]

5-methoxy-1H-benzo[d]imidazole-2-thiol (0.7 g; 1.25equiv.) in an anhydrous acetonitrile was added to a solution of (compound 1**;** 1.0g) and K_2CO_3 (0.75 g; 1.4 equiv.) slowly to the reaction mixture under N_2 medium and was refluxed overnight. The reaction mixture was allowed to cool at r.t., and extracted with EtOAc (3×40 mL) and water. The combined organic layers were washed with brine, dried over Na_2SO_4 and evaporated to yield the crude product which was purified by column chromatography eluted with EtOAc/Hexane (60:40 v/v) to give **Molecule 2** as an off white solid; yield 73%; m.p. 135 ºC; ^{1}H-NMR (400 MHz, DMSO) δ 13.18 (s, 1H, -NH), 8.74 (dd, *J* = 4.0, 1.2 Hz, 1H), 8.39 (s, 1H), 8.37 (d, *J* = 1.6 Hz, 1H), 7.87 (dd, *J* = 7.2, 2.8 Hz, 1H), 7.59 (d, *J* = 6.8 Hz, 2H), 7.51 (dd, *J* = 8.4, 4.4 Hz, 2H), 7.03 (s, 1H), 6.88 (d, *J* = 8.4 Hz, 1H), 6.83 (s, 1H), 3.78 (s, 3H, -OCH_3);^{13}C-NMR (75 MHz, DMSO) δ 170.15, 170.04, 158.26, 157.33, 150.92, 148.28, 140.91, 138.88, 138.48, 136.71, 129.83, 126.99, 126.70, 122.51, 122.01, 120.31, 114.58, 113.04, 103.89, 94.67, 56.00.ESI-MS: m/z =

402.1 [M^++H]; Elemental Anal. Calcdfor $C_{21}H_{15}N_5O_2S$: C, 62.83; H, 3.77; N, 17.45; O, 7.97; S, 7.99; Found: C, 62.25; H, 3.43; N, 17.80; S, 7.87.

Synthesis of 6-((5-methoxy-1H-benzo[d]imidazol-2-yl)thio)-N-(4-methoxyphenyl) pyrimidin-4-amine [Molecule 3]

To a mixture of compound 5-methoxy-1H-benzo[d]imidazole-2-thiol (1 g; 1.3 equiv.) and K_2CO_3(0.87 g; 1.5equiv.) in anhydrous DMF:THF (1:1) under N_2 medium, 6-chloro-N-(4-methoxyphenyl)pyrimidin-4-amine (compound 3**;** 1g) was added slowly and the reaction mixture was reflux overnight. After completion of the reaction as (monitored by TLC), the reaction mixture was allowed to cool at r.t., and extracted with EtOAc (3×50mL) and water. The combined organic layers were washed with brine, dried over Na_2SO_4 and evaporated to yield the crude product which was purified by column chromatography eluted with EtOAc/Hexane (60:40 v/v) to give **Molecule 3** as sunset yellow solid; yield 57%; m.p. 201-202 ºC; ^{1}H NMR (400 MHz, DMSO) δ 13.09 (s, 1H), 9.39 (s, 1H), 8.35 (s, 1H), 7.52 (d, *J* = 8.8 Hz, 2H), 7.35 (d, *J* = 7.2 Hz, 2H), 7.06 (s, 1H), 6.90 (d, *J* = 2.4 Hz, 1H), 6.87 (d, *J* = 2.4 Hz, 1H), 6.79 (d, *J* = 8.8 Hz, 2H), 6.22 (s, 1H), 3.78 (s, 3H), 3.66 (s, 3H);^{13}C-NMR (75 MHz, DMSO) δ 166.29, 160.66, 158.07, 157.35, 156.27, 155.74, 145.28, 139.14, 136.77, 132.53, 130.57, 122.65, 120.39, 114.41, 112.79, 101.41, 94.64, 56.01, 55.62; ESI-MS: m/z = 380.1 [M^++H]; Elemental Anal. Calcd for $C_{19}H_{17}N_5O_2S$: C, 60.14; H, 4.52; N, 18.46; O, 8.43; S, 8.45; Found: C, 60.28; H, 4.31; N,18.44; S, 8.95.

Synthesis of 4-methyl-7-((6-(quinolin-8-yloxy)pyrimidin-4-yl)oxy)-2H-chromen-2one [Molecule 4]

To a mixture of (compound 1**;** 0.75g) and K_2CO_3 (0.4 g; 1.5equiv.) in anhydrous DMF under N_2 medium, 4-methyl-7-hydroxycoumarin (0.61 g; 1.2equiv.) was added drop-wise at r.t. and the reaction mixture was refluxed overnight. After the completion of reaction (observed by TLC), the reaction mixture was allowed to cool at r.t. and extracted with EtOAc (3×40mL). The organic layer was washed with water twice, brine, dried overNa_2SO_4 and evaporated at reduced pressure to yield the crude product which was purified by column chromatography eluted with EtOAc/Hexane (80:20 v/v) to give **Molecule 4** as a pure off white solid; yield 69%;m.p. 185-187 ºC; ^{1}H-NMR (400 MHz, $CDCl_3$) δ 8.85 (dd, *J* = 4.4, 1.6 Hz, 1H, Ar), 8.29 (s, 1H, Ar), 8.21 (d, *J* = 6.8 Hz, 1H, Ar), 7.78 (d, *J* = 6.4 Hz, 1H, Ar), 7.65 – 7.57 (m, 2H, Ar), 7.56 (d, *J* = 1.6 Hz, 1H, Ar), 7.44 (d, *J* = 4.4 Hz, 1H, Ar), 7.17 (s, 1H, Ar), 7.13 (dd, *J* = 8.4, 2.0 Hz, 1H, Ar), 6.63 (s, 1H, Ar), 6.25 (d, *J* = 0.8 Hz, 1H, Ar), 2.42 (s, 3H, -CH_3); ^{13}C-NMR (100 MHz, $CDCl_3$) δ 172.29, 170.59, 160.48, 158.01, 155.16, 154.49, 151.93, 150.58, 148.63, 141.35, 136.25, 129.87, 126.49, 126.17, 125.71, 121.91, 121.54, 118.00, 117.72, 114.41, 110.32, 93.16, 18.76;ESI-MS: m/z = 397.0 $[M]^+$, 398.0 $[M^+$+H]; Elemental Anal. Calcdfor $C_{23}H_{15}N_3O_4$: C, 69.52; H, 3.80; N, 10.57; O, 16.10; Found: C, 69.59, H, 3.53; N, 10.51.

Synthesis of 7-((6-((5-methoxy-1H-benzo[d]imidazol-2-yl)thio)pyrimidin-4-yl)oxy)-4-methyl -2H-chromen-2-one [Molecule 5]

To a solution of (compound 2**;**1.0g) and K_2CO_3 (0.67 g; 1.4 equiv.) in an anhydrous acetonitrile, 5-methoxy-1H-benzo[d]imidazole-2-thiol (0.78 g; 1.25 equiv.) was added slowly under N_2 medium and was refluxed overnight. The reaction mixture was allowed to cool at r.t., extracted with EtOAc (3×40mL) and water. The organic layers were washed with brine, dried over Na_2SO_4 and evaporated to yield the crude product which was purified by column chromatography eluted

with EtOAc/Hexane (60:40 v/v) to give **Molecule 5** as a pure sunset yellow solid; yield 57%.m.p. 195-197 ºC; ^{1}H-NMR (300 MHz, DMSO) δ 13.17 (s, 1H), 8.62 (s, 1H), 7.77 (d, *J* = 8.7 Hz, 1H), 7.55 (s, 1H), 7.31 (d, *J* = 2.1 Hz, 1H), 7.19 (dd, *J* = 8.7, 2.1 Hz, 1H), 7.00 (s, 1H), 6.90 (s, 1H), 6.79 (s, 1H), 6.37 (s, 1H), 3.81 (s, 3H), 3.37 (s, 3H);^{13}C-NMR (75 MHz, DMSO) δ 170.92, 168.88, 159.99, 158.41, 157.23, 154.68, 154.19, 153.20, 138.40, 136.41, 127.04, 120.14, 118.37, 117.91, 114.13, 112.96, 110.15, 104.46, 94.57, 79.57, 55.95, 18.54; ESI-MS: m/z = 433.0 [M^{+}+H], 434.0 [(M^{+}+2H)], 335.0 [(M^{+}+3H)]; Elemental Anal. Calcd for $C_{22}H_{16}N_4O_4S$: C, 61.1; H, 3.73; N, 12.9; O, 14.8; S, 7.41; Found: C, 61.25; H, 3.82; N, 12.54; S, 7.21.

Fluorescence binding studies

Fluorescence measurements were carried out on the Jasco Spectrofluorimeter (Model FP-6200) using 5 mm quartz cuvette. Stock solution (5mg/ml) of synthesized molecules were prepared in the DMSO and then diluted to 1 mg/ml in the 50 mM phosphate buffer pH 7.4 containing 150 mM NaCl (PBS). Intrinsic fluorescence emission spectra of CAMKIV in the presence of different concentrations of synthesized molecules were performed in the PBS at 25°C. For this purpose excitation wavelength was fixed at 280 nm and emission spectra were collected in the range of 300-400 nm. The excitation and emission slit widths (5 nm each) and scan rate (100 nm/min) were constantly maintained for all experiments. A typical emission peak was observed at 343 nm. Final spectrum was collected after deducting their corresponding blank. Three independent experiments were performed for each molecule and their average was taken for data

analyses. A decrease in the fluorescence intensity due to increasing concentrations of ligands were used as a parameter for the calculation of the binding constant *K*a and number of binding sites *n* using the modified Stern-Volmer equations with slight modification [44].

$$\log(F_o\text{-}F)/F = \log K_a + n\log[L] \quad (1)$$

Where, F_o is the fluorescence intensity of protein and F is the fluorescence intensity of ligand, K_a is the binding constant and n is the number of binding sites, [L] represents ligand concentration. For the ligand-protein complex, the values for K_a and *n* can be derived from the intercept and slope, respectively.

MTT assay

To check the biological activity of synthesized compounds, we performed MTT assay on the normal and cancerous human cell lines. In short, exponentially growing HuH7 and HEK293 cells were seeded in a 96-well micro titer plate (approximately 8000 cells per well). In order to check proliferation, cells were treated with increasing concentrations (5 μM-150 μM) of inhibitors on the subsequent day. For both cytotoxicity and activity studies, curcumin was used as a positive control. After 48 hrs of incubation, whole mixture (media + inhibitor) was removed from the cells. After washing the cells two times with PBS, 100μl DMEM and 20 μl MTT (from 5mg/ml stock) was added to each well. The plates were incubated further for 4-5 hrs at 37°C in a CO_2 incubator. As the incubation period was completed, bulk of the residual medium was removed

using a multichannel pipette. Care should be taken to leave the formazan crystals formed behind. To dissolved the formazan crystals, in each well, 100 µl DMSO was added. The plates were then agitated for 15-20 minutes on an orbital plate shaker after which they were read immediately on titerplate reader (BioRad) at 570 nm. The relative cell viabilities (in percentage) were calculated by comparing the viability of the treated cells with that of the control [45].

Propidium iodide assay

Propidium iodide (PI) staining and flow cytometry were used to determine the cell apoptosis and cell cycle stage analysis [46, 47]. HuH7 and HEK293 cell lines were treated with different doses (50, 100 and 200 µM) of molecule 1-3 and compound 2, and doses (50, 100 and 150 µM) of molecule 4, 5 and compound 1 for 48 h at 37ºC, and the control cells were treated with the media only. After harvesting the culture 2 $x10^6$ cells were washed with 5 ml of PBS, and trypsinized at 37ºC for 5–10 min. Cells were centrifuged at 800 rpm for 5 min and washed with 5 ml of PBS. Cells were resuspended in 500µl of PBS and fixed with 4.5 ml of 70% chilled ethanol with gentle mixing and incubated at 4ºC for overnight. Fixed cells were centrifuged at 1500 rpm for 5 min and washed two times with 5 ml PBS. The cells were resuspended in 50µl of PBS, RNase A (200 µg/ml) was added in the dark and incubated for 5 min at 4ºC. 500µl of PI (2µg/ml) was added with 450µl of citrate buffer and incubated for 5 min at 4ºC. 10,000 events for each sample were analyzed by flow cytometry BD FACS Canto and data analysis was performed with FACS DIVA software [48].

Results and Discussion

In the past decade, designing the kinase inhibitor progressed effectively [2, 49]. In addition to the clinical approval of a number of new drugs, efficient approaches for the development of potent and selective inhibitors with a desirable property have become established [50, 51]. CAMKIV is involved in numerous biological activities and acts on broad range of substrates. Transcription factors such as CREB [52], CREMτ [53] and serum response factor [54] are among the best substrates for CAMKIV. This enzyme plays critically important role in the cell proliferation, gene expression, apoptosis, muscle contraction and neurotransmitter release [55-58]. Over-expression or mutation in the CAMKIV causes disruption of transcription activation and signaling which leads to ovarian and lung cancer [22]. Beside disruption of CAMKIV activation, it also causes memory loss and systemic lupus erythematosus [59-61]. Small inhibitory molecules and their binding specificities have been crucial in identifying key roles of CAMKIV inhibitors in health and disease and make an essential molecule to fight against several neurodegenerative diseases and cancer [62].

Docking

Structure-based drug design approach was chosen to design potential inhibitors of CAMKIV [63-65]. The reported crystal structure of human CAMKIV was retrieved from RCSB (PDB ID 2W4O) and further refined before the docking as reported [36]. ParDOCK molecule of *Sanjeevini* drug-design suit was used for docking and scoring. There 100 potential compounds which show admirable binding-affinity to the CAMKIV, were listed in the **Table S1.** We further selected top seven synthesizable molecules which showed significant binding free energy value

with the CAMKIV **(Table 1).** Appreciable docking scores were obtained, indicating a reasonably strong binding affinity of these molecules to the CAMKIV.

We found molecule 1 occupies the active site cavity of CAMKIV **(Figure S1)**. Amino acid Glu168 of CAMKIV forms H-bonds with the molecule 1 supported by several hydrophobic interactions. The binding free energy value of this molecule is –5.60 kcal/mol **(Table 1)** which indicates a moderate binding affinity to the CAMKIV. We further selected a slightly bigger thiol based ligand (molecule 2) which interacts with Ala56 and Gly53 via three H-bonds and several van der Waals interactions **(Figure S2)**. Similarly, binding of molecule 3, compound 2, molecule 4 & 5 are represented in the **Supplementary Figures S3 to S6,** respectively and their binding free energy (ΔG in kcal/mol) is provided in the **Table 1.**

In order to get better inhibitor, we have decreased the size of ligand and designed compound 1 for further study **(Figure 1)**. We found the Asn169 and Asp164 of CAMKIV forms 3 H-bonds with the compound 1 along with several van der Waals interactions **(Figure 1B)**. It is interesting to note that compound 1 penetrated deep inside the active site and forming H-bonded interactions with the active site residue Asp164. On the other hand, hydrophobic residues also play the role in stabilizing the protein-ligand complex by forming an alkyl– π interaction with central pyrimidine ring. A very high binding free-energy (ΔG= –11.52 kcal/mol) was observed for the compound 1 which further indicates its potential binding affinity to the CAMKIV because it completely enters deeper into the active site cavity of CAMKIV **(Figure 1C)**. These observations clearly suggest that compound 1 exhibits strong binding affinity for the CAMKIV and presumably considered as potential inhibitor.

Chemistry

The synthetic routes for all the synthesized molecules were depicted in Scheme 1 & 2 and were named as **compound 1-3** and **molecule 1-5.** These compounds were synthesized involving multi nucleophilic aromatic substitution reactions. At first, the commercially available 4,6-dichloropyrimidine (1) was treated with desired aromatic amine or phenol as nucleophile in the presence of appropriate base in anhydrous dimethylformamide (DMF) or acetonitrile (CH_3CN) from $0^{\circ}C$ to r.t. to obtain mono-substituted compounds 1-3 in a good yield. The formed compounds were further treated with phenol, benzimidazole, etc. in presence of anhydrous DMF, THF or CH_3CN at higher temperature to furnish molecule 1-**5 (Scheme 1 & 2; see the supporting information S17-S20).**

The first as well as second substitution of the nucleophile showed temperature dependent nucleophilic aromatic substitution reaction. The first chlorine of the pyrimidine ring was replaced at 0 ºC to r.t. with 1-1.2 equiv. of nucleophile and 1-1.5 equiv. of appropriate base in an anhydrous DMF while second chlorine replaced at higher temperature with 1-1.2 equiv. of nucleophile and 1.5 equiv. of appropriate base in an anhydrous DMF under dry nitrogen atmosphere. All the synthesized compounds were purified by column chromatographic technique using EtOAc/hexane as an eluent are stable at r.t. Synthesized compounds were confirmed by elemental analysis and further characterized by ^{1}H NMR, ^{13}C NMR and mass spectrometry (ESI-MS) shown in **Supplementary Figures S7-S13 and S14-S20,** respectively.

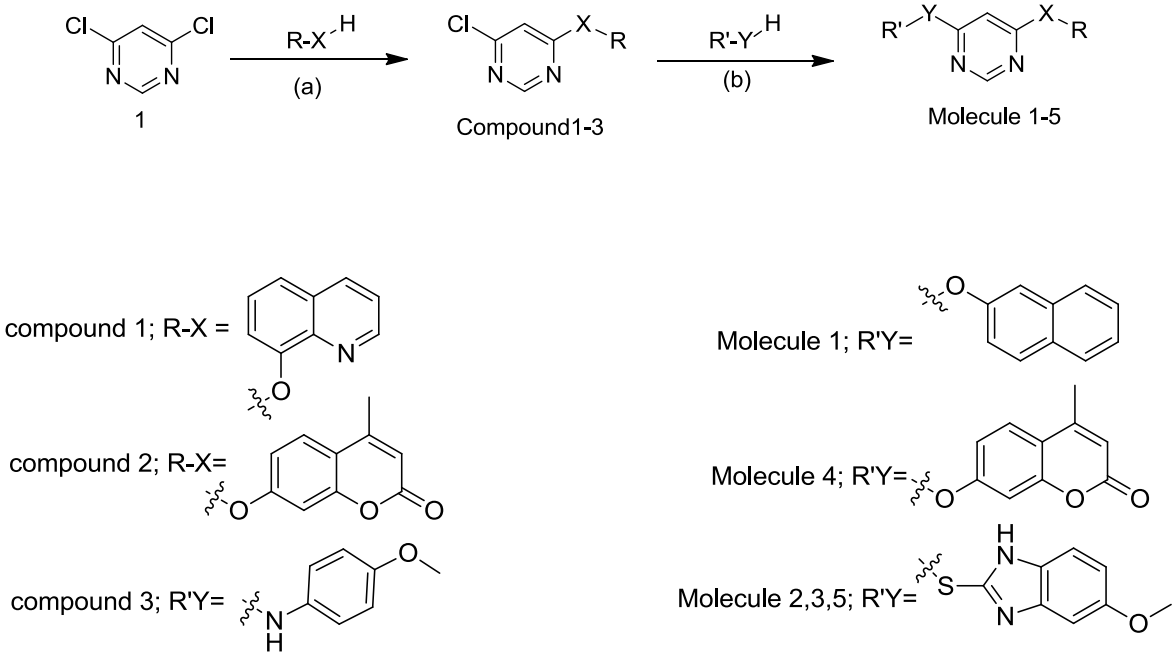

Scheme 1. Synthetic pathway of target molecules 1-7. *Reagents and Conditions*: 1= 4,6-dichloropyrimidine, X= Oxygen and nitrogen containing nucleophile; (a) Appropriate base, room temperature, 3-8 hrs. (b) Appropriate base, anhydrous solvents, overnight reflux, Y= Oxygen and sulphur containing nucleophile.

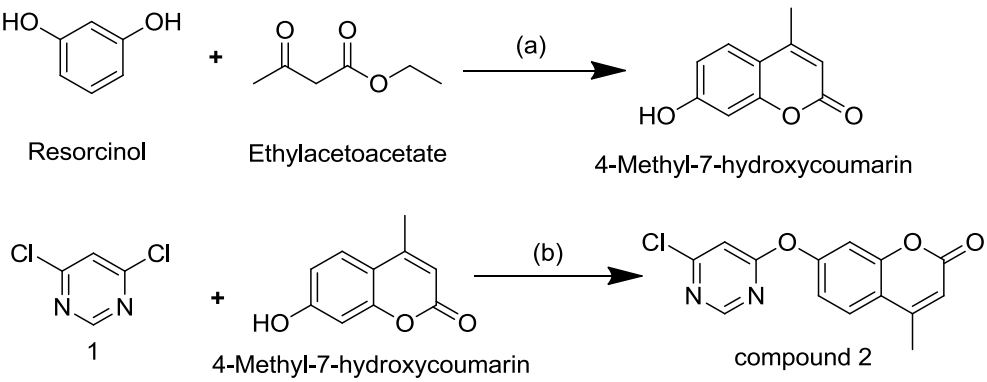

Scheme 2. *Reagents and conditions*: (a) Conc. H_2SO_4, Ice-bath, overnight.1= 4,6-dichloropyrimidine, (b) K_2CO_3, DMF, r.t., 5-6 hrs.

Fluorescence binding studies

CAMKIV has five tryptophan residues which give an emission peak in the range of 300–400 nm once excited at 280 nm [66, 67]. To measure the binding affinity of CAMKIV with designed inhibitors, a 2.0 ml solution containing 2- 4 μM of CAMKIV was titrated by the successive addition of 1.0 mM stock solution of ligands and the concentration were varied from 0 to 108 μM in order to get the saturation. The effect of synthesized compounds on the fluorescence emission spectra of CAMKIV (at pH 7.4 & 27^{o}C) are shown in **Figure 2**. A decrease in the fluorescence intensity by the successive addition of ligands clearly indicates a significant binding of synthesized molecules to the CAMKIV.

The relationship between change in the fluorescence intensity and concentration of ligands was used to calculate the binding constants and the number of binding sites per molecule, as described by the Stern–Volmer equation following equation (1). The apparent *K*a is the binding constant and *n* is the number of binding sites per protein molecule can be expressed for ligand-CAMKIV system [68, 69]. **Figure 2** clearly indicates that all 7 molecules quench the fluorescence emission of CAMKIV with higher binding affinity and experience a static quenching process. The data of fluorescence intensity at 343 nm were plotted against [ligand] to calculate the binding affinity and the number of binding sites shown in the **Figure 3** (for A-G: A=molecule 1; B= molecule 2; C= molecule 3; D= compound 2; E= molecule 4; F= molecule 5; G= compound 1). A liner relation was observed with linear regression 0.99 and binding affinities of compounds 1, 2 and molecules 1-5 were calculated from Stern–Volmer equation listed in the **Table 1**. It is interesting to note that compound 1 shows a significantly high binding affinity for the CAMKIV ($9.2x10^{10}$ M^{-1}(±0.18)) and the number of binding sites *n* is three. This finding is

consistent with the molecular docking results. All these observations clearly indicate that compound 1 is a potent ligand which may be further exploited for the development of novel pharmacophore for the CAMKIV.

MTT assay

MTT is a tetrazolium salt, that is reduced to formazan by reducing enzyme present in metabolically active dividing cells [70]. We have performed MTT assay to analyze the cytotoxicity and cell-proliferation inhibition activity of designed inhibitors. For the cytotoxicity studies, we have used the HEK293 cells. Comparison of the cell viabilities under different treatments is shown in **Figure 4A** (for molecule 1-5) and **4B** (for compound 1 & 2). We found that compound 2 and molecules 1 and 4 are non-toxic till 200 µM concentration while the molecules 2, 3, 5 and compound 1 are non-toxic upto 400 µM to the HEK293 cells **(Table 1).**

To further check the anti-cancer activity of these inhibitors, we used HuH7 and found a significant anticancer activity. Cell proliferation assay with increasing concentrations of molecules 1-5 and compound 1 & 2 are shown in the **Figure 4C and 4D,** respectively. From these data the percentage viability were calculated to estimate the IC_{50} (50% inhibitory concentration) values of each inhibitor **(as shown in Table 1).** Molecule 1, 3-5 and compound 2 show higher IC_{50} values. Whereas, molecule 2 and compound 1 are having the lowest IC_{50} values which suggests that these molecules are more active against cancerous cells. We observed that molecule 2 and compound 1 inhibit the proliferation of cancerous cells almost two times more than the other synthesized molecules. These results are comparable to curcumin, a natural anticancer molecule used a positive control in this study. These outcomes also suggest that such inhibitors are selective and proven 8–10 times more active against cancerous cells then normal

one**.** Moreover, the molecule 2 and compound 1 on HuH7 cells shows the enhanced anti-proliferative activity in comparison to molecule 1,3-5 and compound 2 which was further complimented by binding, docking and cell cycle analysis results.

PI assay

To investigate the apoptotic potential of all seven molecules, both HuH7 and HEK293 were incubated with each molecule with increasing concentrations for 48 h. **Figure 5** shows the percentage of apoptotic cells at 48 h of treatment with compounds 1, 2 and molecules 1-5. In HuH7 cell line, treatment with 50μM of molecules 1-3 and compound 2 induce 1.7%, 2.7%, 1.5% and 1.9% of apoptosis, respectively **(Figure 5A and B)**. At concentrations 100μM of molecules 1-3 and compound 2 the percentage of apoptotic cells were observed 3.5%, 7.6%, 3.1% and 3.8%, respectively. While, at higher concentrations of 200μM of compound molecules 1-3 and compound 2 around 8.6%, 23.6%, 10.1% and 12.5% cells underwent apoptosis. A similar results were observed in case of molecule 4,5 and compound 1, on increasing the concentration of these molecules the percentage of apoptotic cells increase **(Figure 5C and D)**. Maximum apoptosis was observed at 150μM of molecule 4,5 and compound 1 i.e.; 8.2%, 15.8% and 24.5%, respectively in HuH7 cell line.

In HEK293 cell line, all compounds 1, 2 and molecules 1-5 induce a dose-dependent increase in the apoptosis. Molecules 1-3 and compound 2 showed a highest apoptotic potential at concentrations of 200μM and the apoptotic cells were observed 3.8%, 4.3% ,3.4% and 3.8%, respectively at 200μM concentrations **(Figure 6A and B)**. Whereas, molecule 4,5 and compound 1 induce a 4.2%, 4.1% and 6.0% of cells to undergo apoptosis at higher concentrations 150μM **(Figure 6C and D).** Out of seven molecules, molecule 2 and compound 1 are showing best

apoptotic potentials. These two compounds (molecule 2 and compound 1) are significantly ($p<0.0001$) induce apoptosis in HuH7 and HEK293 cell lines. These results further consistent with the MTT assay and florescence binding experiments for molecule 2 and compound 1.

Conclusion

Despite of crucial importance of the CAMKIV in the regulation of vital cellular processes a little attention was given towards the design of potential inhibitors against CAMKIV. Here, we successfully designed seven potential ligands of CAMKIV and performed its cytotoxicity assay, anticancer properties and PI assay. We found compound 1 has the all characteristic features to being considered as a potential pharmacophore. Our studies provided a deeper insight into the identification of potent CAMKIV inhibitors and more towards issues of target selectivity, cellular efficacy, therapeutic effectiveness and tolerability. Furthermore, our structure analysis study has demonstrated a unique structural property of the CAMKIV which provides a molecular basis for understanding towards the distinct selectivity. Inhibition of CAMKIV activity may be useful for the blocking of phosphorylation activity or by disrupting protein-protein interactions which in turn facilitate the interruption of various cellular cascades. Finally, our findings on novel potential inhibitors open a promising channel towards to application of pyrimidine derivative for the treatment of ailments associated with CAMKIV.

Acknowledgements

This work is funded by Indian Council of Medical Research, Government of India. NH thanks Prof. B. Jayaram for providing computational biology facility, SCFBio Indian Institute of Technology, New Delhi. HN and JK thank to the Indian Council of Medical Research and Council of Scientific and Industrial Research (India), respectively for the award of senior research fellowships. We sincerely acknowledge Harvard University-plasmid providing facility for providing the *CAMK4* gene. Authors thank to the Department of Science and Technology, Government of India for the FIST support (FIST program No. SR/FST/LSI-541/2012).

Conflict of Interest

The authors have no conflicts of interest with the current work or its publication.

References

1. Roskoski R (2015) A historical overview of protein kinases and their targeted small molecule inhibitors. *Pharmacological Research;***100**: 1-23.

2. Zhang J, Yang PL, Gray NS (2009) Targeting cancer with small molecule kinase inhibitors. *Nat Rev Cancer;***9**: 28-39.

3. Manning G, Whyte DB, Martinez R, Hunter T, Sudarsanam S (2002) The protein kinase complement of the human genome. *Science;***298**: 1912-34.

4. Hainaut P, Plymoth A (2013) Targeting the hallmarks of cancer: towards a rational approach to next-generation cancer therapy. *Curr Opin Oncol;***25**: 50-1.

5. Hanahan D, Weinberg RA (2011) Hallmarks of cancer: the next generation. *Cell;***144**: 646-74.

6. Wu P, Nielsen TE, Clausen MH (2016) Small-molecule kinase inhibitors: an analysis of FDA-approved drugs. *Drug Discov Today;***21**: 5-10.

7. Wu P, Nielsen TE, Clausen MH (2015) FDA-approved small-molecule kinase inhibitors. *Trends Pharmacol Sci;***36**: 422-39.

8. Tokumitsu H, Enslen H, Soderling TR (1995) Characterization of a Ca2+/calmodulin-dependent protein kinase cascade. Molecular cloning and expression of calcium/calmodulin-dependent protein kinase kinase. *J Biol Chem;***270**: 19320-4.

9. Krebs J (1998) Calmodulin-dependent protein kinase IV: regulation of function and expression. *Biochim Biophys Acta;***1448**: 183-9.

10. Tokumitsu H, Brickey DA, Glod J, Hidaka H, Sikela J, Soderling TR (1994) Activation mechanisms for Ca2+/calmodulin-dependent protein kinase IV. Identification of a brain CaM-kinase IV kinase. *J Biol Chem;***269**: 28640-7.

11. Miyano O, Kameshita I, Fujisawa H (1992) Purification and characterization of a brain-specific multifunctional calmodulin-dependent protein kinase from rat cerebellum. *J Biol Chem;***267**: 1198-203.

12. Wu JY, Means AR (2000) Ca(2+)/calmodulin-dependent protein kinase IV is expressed in spermatids and targeted to chromatin and the nuclear matrix. *J Biol Chem;***275**: 7994-9.

13. Blaeser F, Ho N, Prywes R, Chatila TA (2000) Ca(2+)-dependent gene expression mediated by MEF2 transcription factors. *J Biol Chem;***275**: 197-209.

14. Naz H, Islam A, Ahmad F, Hassan MI (2016) Calcium/calmodulin-dependent protein kinase IV: A multifunctional enzyme and potential therapeutic target. *Prog Biophys Mol Biol;***121**: 54-65.

15. Sheng M, Thompson MA, Greenberg ME (1991) CREB: a Ca(2+)-regulated transcription factor phosphorylated by calmodulin-dependent kinases. *Science;***252**: 1427-30.

16. Sun P, Enslen H, Myung PS, Maurer RA (1994) Differential activation of CREB by Ca2+/calmodulin-dependent protein kinases type II and type IV involves phosphorylation of a site that negatively regulates activity. *Genes Dev;***8**: 2527-39.

17. Silva AJ, Kogan JH, Frankland PW, Kida S (1998) CREB and memory. *Annu Rev Neurosci;***21**: 127-48.

18. Impey S, Fong AL, Wang Y, Cardinaux JR, Fass DM, Obrietan K, et al. (2002) Phosphorylation of CBP mediates transcriptional activation by neural activity and CaM kinase IV. *Neuron;***34**: 235-44.

19. Lin F, Marcelo KL, Rajapakshe K, Coarfa C, Dean A, Wilganowski N, et al. (2015) The camKK2/camKIV relay is an essential regulator of hepatic cancer. *Hepatology;***62**: 505-20.

20. Wu JY, Gonzalez-Robayna IJ, Richards JS, Means AR (2000) Female fertility is reduced in mice lacking Ca2+/calmodulin-dependent protein kinase IV. *Endocrinology;***141**: 4777-83.

21. Williams CL, Phelps SH, Porter RA (1996) Expression of Ca2+/calmodulin-dependent protein kinase types II and IV, and reduced DNA synthesis due to the Ca2+/calmodulin-dependent protein kinase inhibitor KN-62 (1-[N,O-bis(5-isoquinolinesulfonyl)-N-methyl-L-tyrosyl]-4-phenyl piperazine) in small cell lung carcinoma. *Biochem Pharmacol;***51**: 707-15.

22. Knapp S, Sundstrom M (2014) Recently targeted kinases and their inhibitors-the path to clinical trials. *Curr Opin Pharmacol;***17**: 58-63.

23. Sumi M, Kiuchi K, Ishikawa T, Ishii A, Hagiwara M, Nagatsu T, et al. (1991) The newly synthesized selective Ca2+/calmodulin dependent protein kinase II inhibitor KN-93 reduces dopamine contents in PC12h cells. *Biochem Biophys Res Commun;***181**: 968-75.

24. Tokumitsu H, Chijiwa T, Hagiwara M, Mizutani A, Terasawa M, Hidaka H (1990) KN-62, 1-[N,O-bis(5-isoquinolinesulfonyl)-N-methyl-L-tyrosyl]-4-phenylpiperazi ne, a specific inhibitor of Ca2+/calmodulin-dependent protein kinase II. *J Biol Chem;***265**: 4315-20.

25. Zhang X, Wheeler D, Tang Y, Guo L, Shapiro RA, Ribar TJ, et al. (2008) Calcium/calmodulin-dependent protein kinase (CaMK) IV mediates nucleocytoplasmic shuttling and release of HMGB1 during lipopolysaccharide stimulation of macrophages. *J Immunol;***181**: 5015-23.

26. Pellicena P, Schulman H (2014) CaMKII inhibitors: from research tools to therapeutic agents. *Front Pharmacol;***5**: 21.

27. Bates SE, Amiri-Kordestani L, Giaccone G (2012) Drug development: portals of discovery. *Clin Cancer Res;***18**: 23-32.

28. Hassan MI, Kumar V, Singh TP, Yadav S (2007) Structural model of human PSA: a target for prostate cancer therapy. *Chem Biol Drug Des;***70**: 261-7.

29. Hassan MI, Kumar V, Somvanshi RK, Dey S, Singh TP, Yadav S (2007) Structure-guided design of peptidic ligand for human prostate specific antigen. *J Pept Sci;***13**: 849-55.

30. Naz F, Shahbaaz M, Bisetty K, Islam A, Ahmad F, Hassan MI (2015) Designing New Kinase Inhibitor Derivatives as Therapeutics Against Common Complex Diseases: Structural Basis of Microtubule Affinity-Regulating Kinase 4 (MARK4) Inhibition. *OMICS;***19**: 700-11.

31. Naz F, Shahbaaz M, Khan S, Bisetty K, Islam A, Ahmad F, et al. (2015) PKR-inhibitor binds efficiently with human microtubule affinity-regulating kinase 4. *J Mol Graph Model;***62**: 245-52.

32. Kumari S, Idrees D, Mishra CB, Prakash A, Wahiduzzaman, Ahmad F, et al. (2016) Design and synthesis of a novel class of carbonic anhydrase-IX inhibitor 1-(3-(phenyl/4-fluorophenyl)-7-imino-3H-[1,2,3]triazolo[4,5d]pyrimidin 6(7H)yl)urea. *J Mol Graph Model;***64**: 101-9.

33. Shahbaaz M, Bisetty K, Ahmad F, Hassan MI (2016) Current Advances in the Identification and Characterization of Putative Drug and Vaccine Targets in the Bacterial Genomes. *Curr Top Med Chem;***16**: 1040-69.

34. Thakur PK, Hassan I (2011) Discovering a potent small molecule inhibitor for gankyrin using de novo drug design approach. *Int J Comput Biol Drug Des;***4**: 373-86.

35. Thakur PK, Kumar J, Ray D, Anjum F, Hassan MI (2013) Search of potential inhibitor against New Delhi metallo-beta-lactamase 1 from a series of antibacterial natural compounds. *J Nat Sci Biol Med;***4**: 51-6.

36. Hoda N, Naz H, Jameel E, Shandilya A, Dey S, Hassan MI, et al. (2015) Curcumin specifically binds to the human calcium-calmodulin-dependent protein kinase IV: fluorescence and molecular dynamics simulation studies. *J Biomol Struct Dyn;*1-13.

37. Naz H, Jameel E, Hoda N, Shandilya A, Khan P, Islam A, et al. (2016) Structure guided design of potential inhibitors of human calcium-calmodulin dependent protein kinase IV containing pyrimidine scaffold. *Bioorg Med Chem Lett;***26**: 782-8.

38. Naz H, Shahbaaz M, Bisetty K, Islam A, Ahmad F, Hassan MI (2016) Effect of pH on the structure, function, and stability of human calcium/calmodulin-dependent protein kinase IV: combined spectroscopic and MD simulation studies. *Biochem Cell Biol;***94**: 221-8.

39. Naz H, Shahbaaz M, Haque MA, Bisetty K, Islam A, Ahmad F, et al. (2016) Urea-induced denaturation of human calcium/calmodulin-dependent protein kinase IV: a combined spectroscopic and MD simulation studies. *J Biomol Struct Dyn;*1-13.

40. Jain T, Jayaram B (2005) An all atom energy based computational protocol for predicting binding affinities of protein-ligand complexes. *FEBS Lett;***579**: 6659-66.

41. Pearlman DA, Case DA, Caldwell JW, Ross WS, Cheatham Iii TE, DeBolt S, et al. (1995) AMBER, a package of computer programs for applying molecular mechanics, normal mode analysis, molecular dynamics and free energy calculations to simulate the structural and energetic properties of molecules. *Computer Physics Communications;***91**: 1-41.

42. Gupta A, Gandhimathi A, Sharma P, Jayaram B (2007) ParDOCK: an all atom energy based Monte Carlo docking protocol for protein-ligand complexes. *Protein Pept Lett;***14**: 632-46.

43. Bhattacharyya SS, Paul S, Mandal SK, Banerjee A, Boujedaini N, Khuda-Bukhsh AR (2009) A synthetic coumarin (4-methyl-7 hydroxy coumarin) has anti-cancer potentials against DMBA-induced skin cancer in mice. *Eur J Pharmacol;***614**: 128-36.

44. Wang YQ, Zhang HM, Zhang GC, Tao WH, Fei ZH, Liu ZT (2007) Spectroscopic studies on the interaction between silicotungstic acid and bovine serum albumin. *J Pharm Biomed Anal;***43**: 1869-75.

45. Bava SV, Puliappadamba VT, Deepti A, Nair A, Karunagaran D, Anto RJ (2005) Sensitization of taxol-induced apoptosis by curcumin involves down-regulation of nuclear factor-

kappaB and the serine/threonine kinase Akt and is independent of tubulin polymerization. *J Biol Chem;***280**: 6301-8.

46. Rieger AM, Nelson KL, Konowalchuk JD, Barreda DR (2011) Modified annexin V/propidium iodide apoptosis assay for accurate assessment of cell death. *J Vis Exp;*

47. Cecchini MJ, Amiri M, Dick FA (2012) Analysis of cell cycle position in mammalian cells. *JoVE (Journal of Visualized Experiments);*e3491-e.

48. Picot J, Guerin CL, Le Van Kim C, Boulanger CM (2012) Flow cytometry: retrospective, fundamentals and recent instrumentation. *Cytotechnology;***64**: 109-30.

49. Kaur M, Singh M, Silakari O (2014) Insight into the therapeutic aspects of 'Zeta-Chain Associated Protein Kinase 70 kDa' inhibitors: a review. *Cell Signal;***26**: 2481-92.

50. Zhao Z, Wu H, Wang L, Liu Y, Knapp S, Liu Q, et al. (2014) Exploration of type II binding mode: A privileged approach for kinase inhibitor focused drug discovery? *ACS Chem Biol;***9**: 1230-41.

51. Abel RL, Haigis MC, Park C, Raines RT (2002) Fluorescence assay for the binding of ribonuclease A to the ribonuclease inhibitor protein. *Anal Biochem;***306**: 100-7.

52. Matthews RP, Guthrie CR, Wailes LM, Zhao X, Means AR, McKnight GS (1994) Calcium/calmodulin-dependent protein kinase types II and IV differentially regulate CREB-dependent gene expression. *Mol Cell Biol;***14**: 6107-16.

53. Sun Z, Sassone-Corsi, P., Means, A.R. (1995) Calspermin gene transcription is regulated by two cyclic AMP response elements contained in an alternative promoter in the calmodulin kinase IV gene. *Molecular and Cellular Biology;***15**: 561-71.

54. Miranti CK, Ginty, D.D., Huang, G., Chatila, T., Greenberg, M.E. (1995) Calcium activates serum response factor-dependent transcription by a Ras- and Elk-1-independent mechanism that involves a Ca2+/calmodulin-dependent kinase. *Molecular and Cellular Biology;***15**: 3672-84.

55. Bachs O, Agell N, Carafoli E (1992) Calcium and calmodulin function in the cell nucleus. *Biochim Biophys Acta;***1113**: 259-70.

56. Lu KP, Hunter T (1995) The NIMA kinase: a mitotic regulator in Aspergillus nidulans and vertebrate cells. *Prog Cell Cycle Res;***1**: 187-205.

57. Nicotera P, Zhivotovsky B, Orrenius S (1994) Nuclear calcium transport and the role of calcium in apoptosis. *Cell Calcium;***16**: 279-88.

58. Bito H, Deisseroth K, Tsien RW (1997) Ca2+-dependent regulation in neuronal gene expression. *Curr Opin Neurobiol;***7**: 419-29.

59. Fukushima H, Maeda R, Suzuki R, Suzuki A, Nomoto M, Toyoda H, et al. (2008) Upregulation of calcium/calmodulin-dependent protein kinase IV improves memory formation and rescues memory loss with aging. *J Neurosci;***28**: 9910-9.

60. Juang YT, Wang Y, Solomou EE, Li Y, Mawrin C, Tenbrock K, et al. (2005) Systemic lupus erythematosus serum IgG increases CREM binding to the IL-2 promoter and suppresses IL-2 production through CaMKIV. *J Clin Invest;***115**: 996-1005.

61. Ichinose K, Rauen T, Juang YT, Kis-Toth K, Mizui M, Koga T, et al. (2011) Cutting edge: Calcium/Calmodulin-dependent protein kinase type IV is essential for mesangial cell proliferation and lupus nephritis. *J Immunol;***187**: 5500-4.

62. Cohen P (2002) Protein kinases--the major drug targets of the twenty-first century? *Nat Rev Drug Discov;***1**: 309-15.

63. Hassan MI (2016) Editorial. Recent Advances in the Structure-Based Drug Design and Discovery. *Curr Top Med Chem;***16**: 899-900.

64. Khan FI, Wei DQ, Gu KR, Hassan MI, Tabrez S (2016) Current updates on computer aided protein modeling and designing. *Int J Biol Macromol;***85**: 48-62.

65. Ferreira LG, Dos Santos RN, Oliva G, Andricopulo AD (2015) Molecular docking and structure-based drug design strategies. *Molecules;***20**: 13384-421.

66. Matveeva EG, Morisseau C, Goodrow MH, Mullin C, Hammock BD (2009) Tryptophan fluorescence quenching by enzyme inhibitors as a tool for enzyme active site structure investigation: epoxide hydrolase. *Curr Pharm Biotechnol;***10**: 589-99.

67. Ino T, Nishioka T, Miyoshi H (2003) Characterization of inhibitor binding sites of mitochondrial complex I using fluorescent inhibitor. *Biochimica et Biophysica Acta (BBA)-Bioenergetics;***1605**: 15-20.

68. Garg A, Manidhar DM, Gokara M, Malleda C, Suresh Reddy C, Subramanyam R (2013) Elucidation of the binding mechanism of coumarin derivatives with human serum albumin. *PloS one;***8**: e63805.

69. Agudelo D, Bourassa P, Bruneau J, Berube G, Asselin E, Tajmir-Riahi HA (2012) Probing the binding sites of antibiotic drugs doxorubicin and N-(trifluoroacetyl) doxorubicin with human and bovine serum albumins. *PloS one;***7**: e43814.

70. Mosmann T (1983) Rapid colorimetric assay for cellular growth and survival: application to proliferation and cytotoxicity assays. *J Immunol Methods;***65**: 55-63.

Supporting Information

Additional Supporting Information may be found in the online version of this article:

Figures S1-S6: Binding mode of molecules 1-5 & compound 2 with the CAMKIV

Figures S7-S13: ^{1}H-NMR and^{13}C NMR spectra of Compounds 1-2 & Molecules 1-5.

Figures S14-S20: Mass spectra of Compounds 1-2 & Molecules 1-5.

Table S1: Binding free energy of the designed compounds with CAMKIV.

Figure Legends

Figure 1: Binding mode of compound 1 with the CAMKIV. (A). Structure of 8-((6-chloropyrimidine-4-yl)oxy)quinoline. **(B).** Showing interaction of the ligand (stick model) with the protein residues Asn169 and Asp164 (orange color stick model). **(C).** Showing surface view of ligand (stick model) present in the active site cavity of the CAMKIV protein.

Figure 2: Fluorescence binding studies of synthesized compounds with the CAMKIV. Figure A to G (for A-G: A=molecule 1; B= molecule 2; C= molecule 3; D= compound 2; E= molecule 4; F= molecule 5; G= compound 1) represent fluorescence emission spectra with CAMKIV.

Figure 3: Modified Stern–Volmer plot for fluorescence quenching of CAMKIV presented in A to G (for A-G: A=molecule 1; B= molecule 2; C= molecule 3; D= compound 2; E= molecule 4; F= molecule 5; G= compound 1), for the calculation of binding affinities.

Figure 4: MTT assay of **(A).** Molecule 1-5 and **(B).** Compound 1 & 2 on HEK293 cells. A total of 8000 cells in triplicates were exposed to the indicated concentration of inhibitors for 48 h and subjected to MTT assay. **(C).** Anti-proliferation assay Molecule 1-5 and **(D).** Compound 1 & 2 on HuH7 cells. A total of 8000 cells in triplicates were exposed to the indicated concentrations of inhibitors for 48 h and subjected to MTT assay. Data represent three independent tests of experiments and results are shown as the mean ± SD. Curcumin is used as a positive control.

Figure 5: PI assay of **(A)**. Molecule 1-3 & Compound 2 indicate its role in the apoptosis on the HuH7 cell line. **(B).** Bar graphs of Molecule 1-3 & Compound 2 represent the mean values of triplicate determinations ± SD. *p < 0.05; **p < 0.01, **p <0.005; ***p <0.0005 compared with the control. PI assay of **(C)**. Molecule 4,5 & Compound 1 indicate its role in the apoptosis on the HuH7cell line. **(B).** Bar graphs of Molecule 4,5 & Compound 1 represent the mean values of triplicate determinations ± SD. *p < 0.05; **p < 0.01, **p <0.005; ***p <0.0005 compared with the control. Data analysis was performed with FACS DIVA software. Statistical analysis was done using Student's t test for unpaired samples.

Figure 6: PI assay of **(A)**. Molecule 1-3 & Compound 2 indicate its role in the apoptosis on the HEK293 cell line. **(B).** Bar graphs of Molecule 1-3 & Compound 2 represent the mean values of triplicate determinations ± SD. *p < 0.05; **p < 0.01, **p <0.005; ***p <0.0005 compared with the control. PI assay of **(C)**. Molecule 4, 5 & Compound 1 indicate its role in the apoptosis on the HEK293 cell line. **(B).** Bar graphs of Molecule 4,5 & Compound 1 represent the mean values of triplicate

determinations ± SD. *p < 0.05; **p < 0.01, **p <0.005; ***p <0.0005 compared with the control. Data analysis was performed with FACS DIVA software. Statistical analysis was done using Student's t test for unpaired samples.

Table 1: Calculated binding free energies, binding affinities and observed IC_{50} values of synthesized

S. No.	Compound	[a]ΔG kcal mol^{-1}	[b]Binding constant	No. of Binding site	[c]IC_{50} (HuH7 cells) in μM	[c]IC_{50} (HEK293 cells) in μM
1.	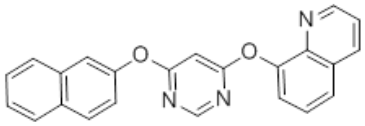 Molecule 1	−5.60	1.5×10^{3}, M^{-1} (±0.15)	1.0	55 ± 1.50	380 ± 1.21
2.	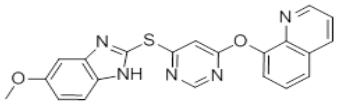 Molecule 2	−7.38	4.1×10^{4}, M^{-1} (±0.20)	1.0	40 ± 1.11	>400
3.	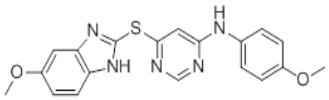 Molecule 3	−7.62	9.9×10^{4}, M^{-1} (±0.18)	1.0	60 ± 1.10	>400
4.	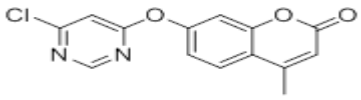 Compound 2	−8.42	2.8×10^{5}, M^{-1} (±0.15)	1.0	124 ± 1.59	330 ± 1.18
5.	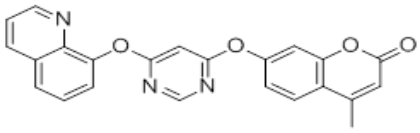 Molecule 4	−11.05	6.9×10^{5}, M^{-1} (±0.19)	1.0	72 ± 1.14	350 ± 1.11
6.	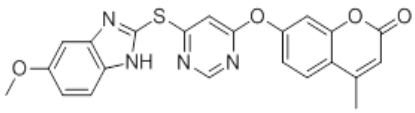 Molecule 5	−11.33	7.4×10^{5}, M^{-1} (±0.16)	1.0	54 ± 1.55	>400
7.	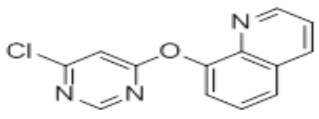 Compound 1	−11.52	9.2×10^{10}, M^{-1}(±0.18)	3.0	39± 1.03	>400

molecules.

a. Calculated from docking, b. Calculated from fluorescence measurements, c. calculated from MTT assay

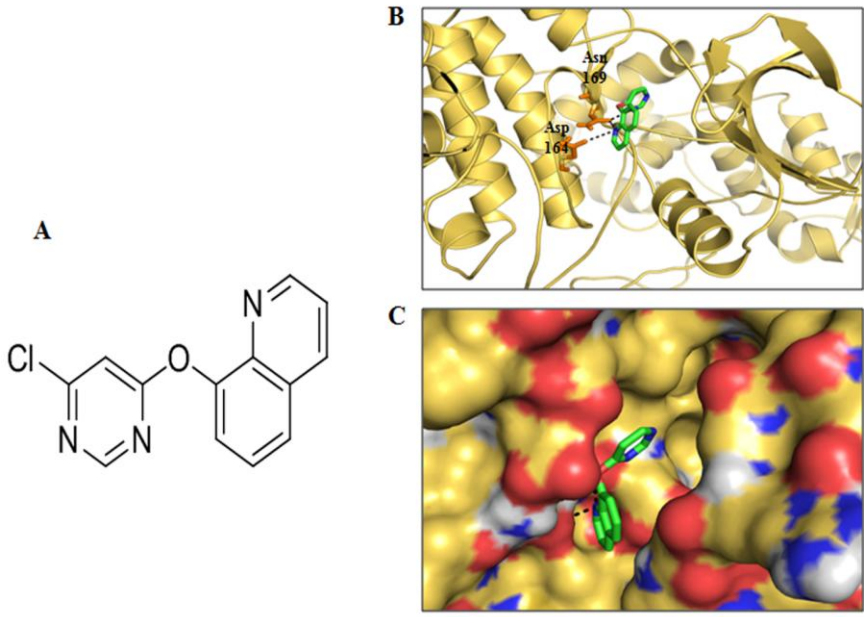

Figure 1

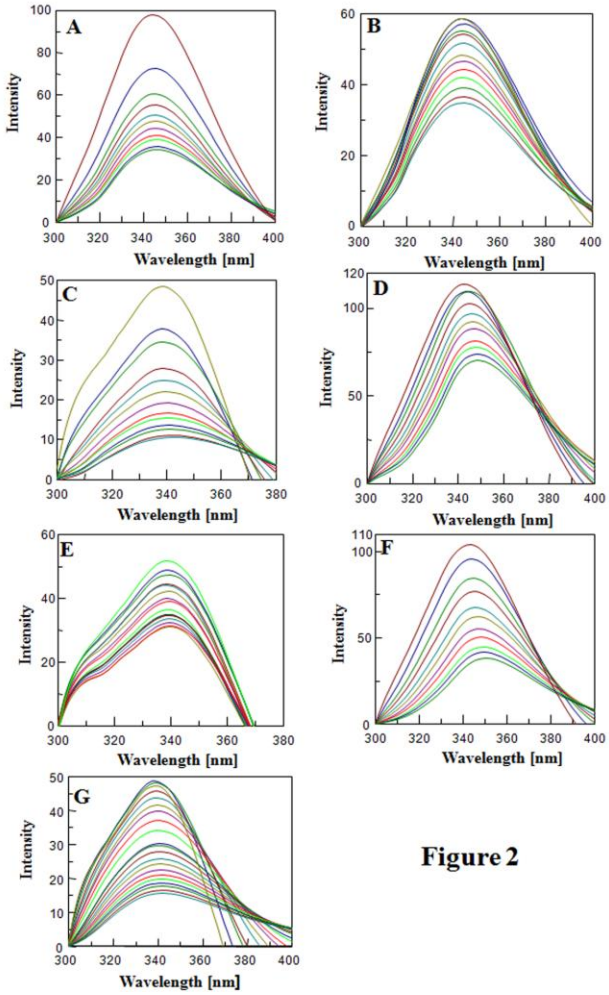

Figure 2

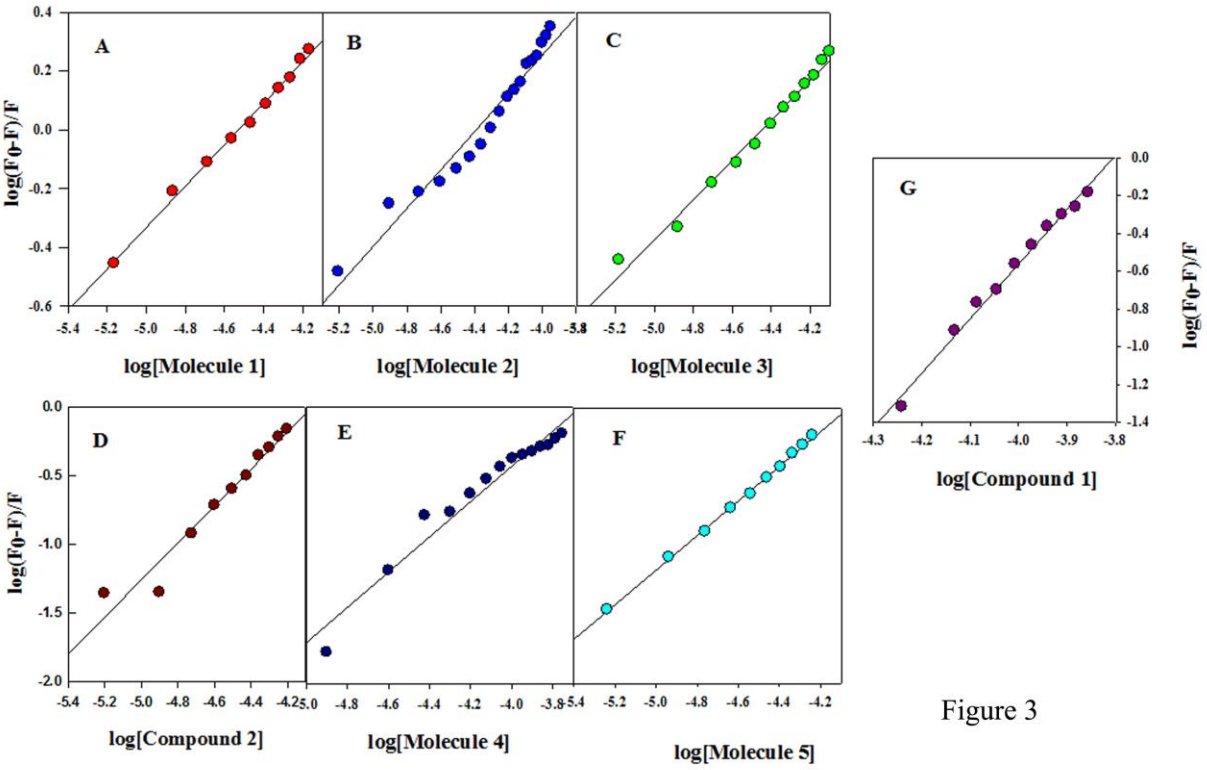

Figure 3

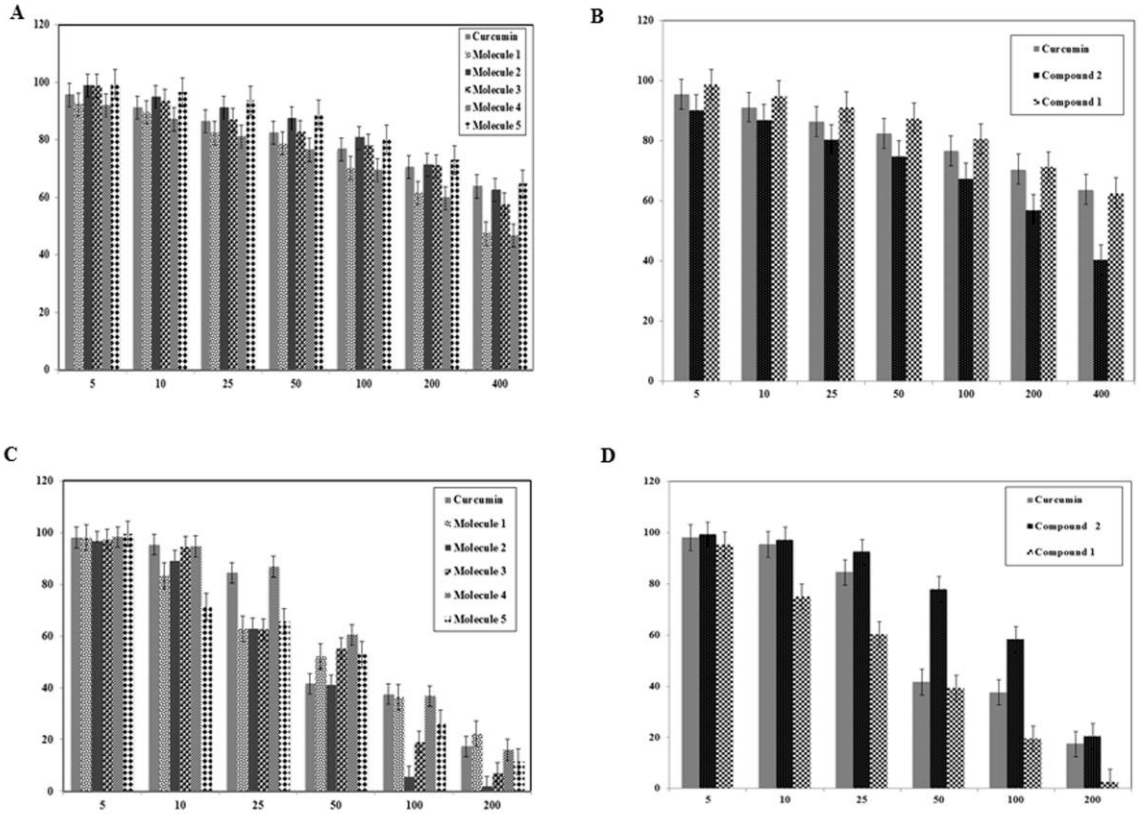

Figure 4

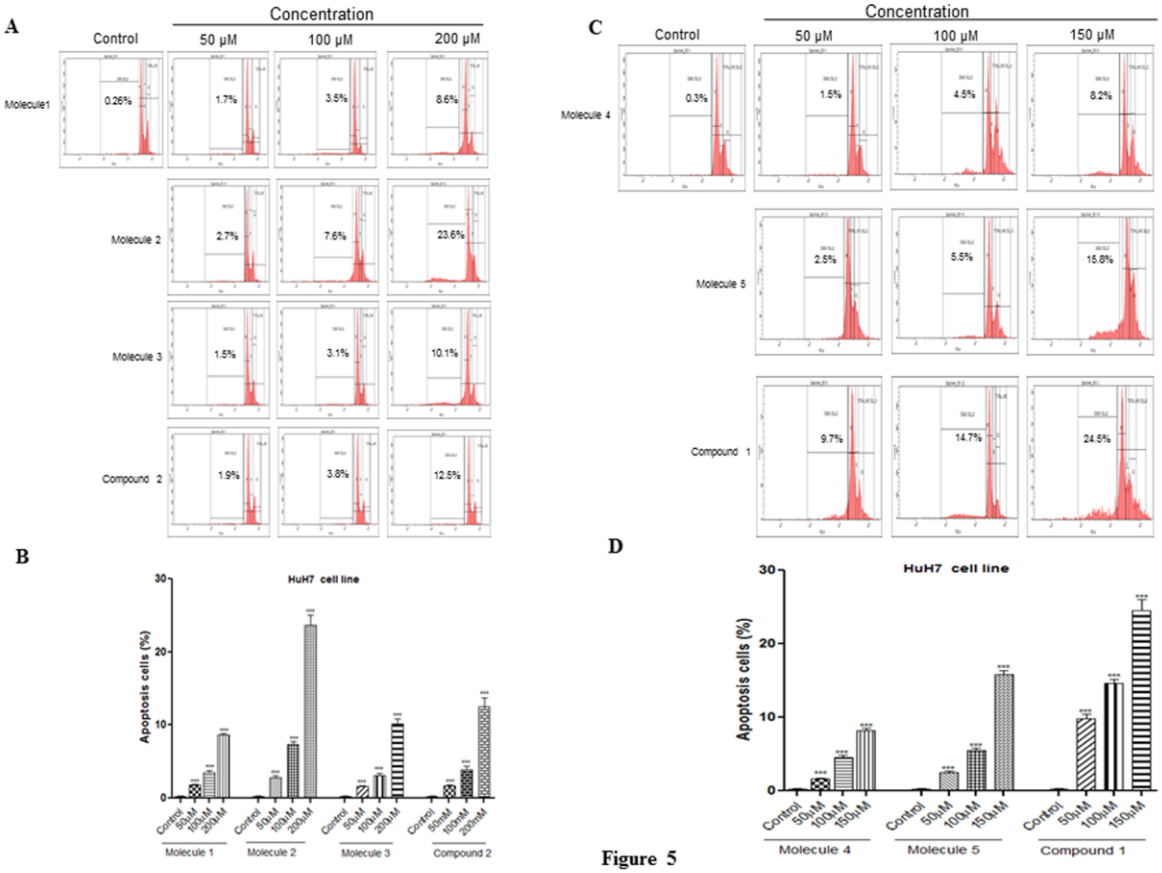

Figure 5

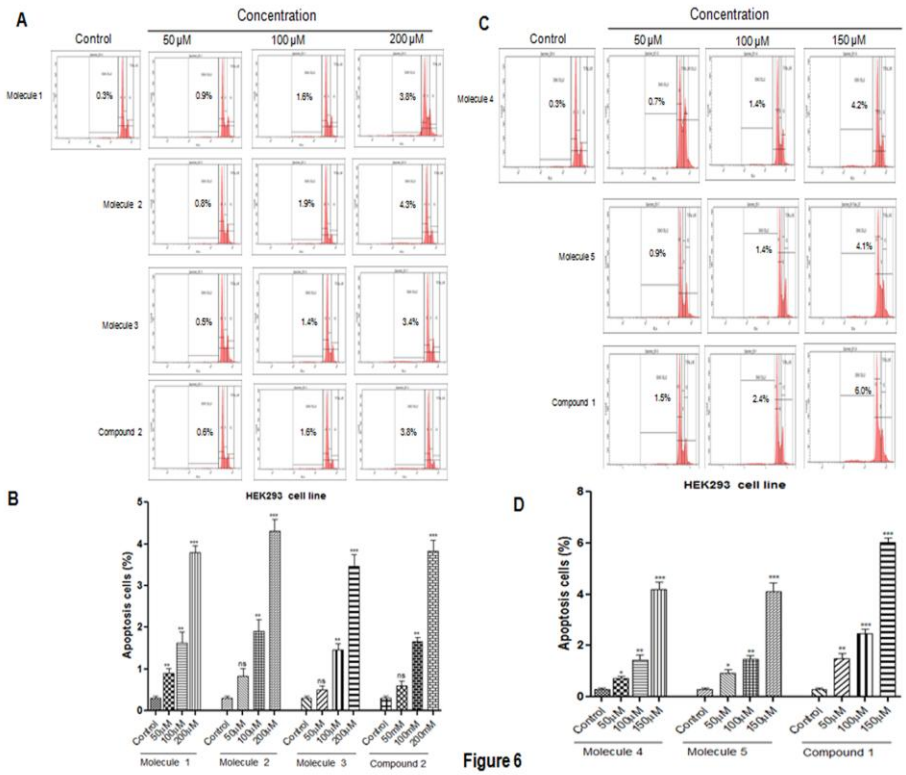

Figure 6